Hyperfine Interactions (2020) 241:54
https://doi.org/10.1007/s10751-020-01719-x

Spin-crossover phenomenon and intermolecular interaction for the assembled Fe(II) complexes having aromatic rings

Saki Iwai [1] **· Satoru Nakashima** [1,2]

Abstract

Assembled Fe(II) complex, $[Fe(NCS)_2(1,5\text{-bpna})_2 \cdot (0.6CH_2Cl_2)(C_2H_5OH)]_n$ (powder sample) (1,5-bpna = 1,5-bis(4-pyridyl)naphthalene), was synthesized. The powder sample showed slight decrease in magnetic susceptibility with decreasing temperature. Small amount of low-spin state was observed in Mössbauer spectrum at 78 K for the powder sample, suggesting incomplete spin-crossover phenomenon. Single crystal of $[Fe(NCS)_2(1,5\text{-bpna})_2 \cdot (\text{toluene})]_n$ was obtained. Magnetic susceptibility for $[Fe(NCS)_2(1,5\text{-bpna})_2 \cdot (\text{toluene})]_n$ revealed high-spin state at all temperature region. X-ray structural analysis revealed the CH-π interaction between bridging ligand and guest toluene. Such interaction forced parallel structure around iron atom, which inhibits the decrease in Fe-N distance to become low-spin state.

Keywords Spin-crossover phenomenon · Assembled complexes · Aromatic ring · CH-π interaction · Local structure around iron atom

1 Introduction

Fe(II) octahedral assembled complexes, $[Fe(NCS)_2(\text{bridging ligand})_2]_n$, can take two spin (high-spin (HS) and low-spin (LS)) states and spin-crossover (SCO) phenomenon appears between the two spin states by external stimuli, such as temperature, pressure, and light-illumination, in intermediate ligand field [1, 2]. The assembled complexes are divided into the

---

This article is part of the Topical Collection on *Proceedings of the International Conference on the Applications of the Mössbauer Effect (ICAME 2019), 1–6 September 2019, Dalian, China*
Edited by Tao Zhang, Junhu Wang and Xiaodong Wang

✉ Satoru Nakashima
snaka@hiroshima-u.ac.jp

[1] Graduate School of Science, Hiroshima University, 1-3-1, Kagamiyama, Higashi-Hiroshima 739-8526, Japan

[2] Natural Science Center for Basic Research and Development, Hiroshima University, 1-4-2, Kagamiyama, Higashi-Hiroshima 739-8526, Japan

complexes exhibiting SCO phenomenon and the complexes not exhibiting it. There is a difference in the local structure around iron atom between them. It has been revealed that SCO phenomenon occurs when the coordinating pyridines facing to each other across the iron atom are propeller type (SCO-on), while the phenomenon does not occur when they are parallel type or distorted propeller type (SCO-off) [3, 4]. When the spin state changes from HS to LS, the Fe-N distance decreases by about 10%. Therefore, local structure around iron atom becomes important to become LS. If the local structure is crowded, the LS state will be destabilized. The results are supported by the theoretical study [3, 4].

Assembled Fe(II) complexes bridged by 1,4-bis(4-pyridyl)benzene show SCO [5], while the complexes bridged by 9,10-bis(4-pyridyl)anthracene do not show it [6]. The difference was thought to be due to the difference in intermolecular interaction [6]. The naphthalene has an intermediate π-system between benzene and anthracene. In the present study, iron (II) assembled complexes, $[Fe(NCS)_2(1,5\text{-bpna})_2]_n$ (1,5-bpna = 1,5-bis(4-pyridyl)naphthalene, Scheme 1), were synthesized and we checked the spin state to reveal the effect of intermolecular interaction on SCO. X-ray structural analysis of $[Fe(NCS)_2(1,5\text{-bpna})_2\cdot(\text{toluene})]_n$ revealed CH-π interaction between guest toluene and bridging ligand to force the local structure around iron atom to be parallel type.

2 Experimental

The 1,5-bpna was synthesized by Suzuki-Miyaura cross-coupling reaction of 4-pyridyl boronic acid with 1/3 equivalent 1,5-dibromonaphthalene. Toluene and water (1:1, *v*/*v*) were used as solvent. [1,1'-Bis(diphenylphosphino)ferrocene]dichloropalladium was used as palladium catalyst and Na_2CO_3 was used as base. The reaction mixture was refluxed for 96 h in the three neck flask under inactive gas atmosphere. Toluene and water were separated using separating funnel and toluene solution was washed with a small amount of water and dried over $MgSO_4$. After filtration, solution was concentrated and the product was purified by alumina column chromatography (eluent: toluene) and recrystallization with toluene. 10% (*v*/*v*) water was added to alumina to reduce its activity. As the result, 1,5-bpna was obtained as brown crystal (yield: 58.5%). Anal. Calcd for $C_{20}H_{14}N_2$: C, 85.08; H, 5.00; N, 9.92%. Found for 1,5-bpna: C, 85.07; H, 5.28; N, 9.88%. ^{1}H NMR ($CDCl_3$): δ 8.76 (q, 4H, PyHα), 7.89 (d, 2H, naph$H_{4,8}$), 7.54 (t, 2H, naph$H_{3,7}$), 7.46 (d, 2H, naph$H_{2,6}$), 7.45 (q, 4H, PyH_β) ppm.

Assembled Fe(II) complex was synthesized by direct mixing method. $FeSO_4\cdot 7H_2O$ (0.2 mmol) and KNCS (0.4 mmol) were dissolved in EtOH (10 mL). The 1,5-bpna (0.4 mmol) was dissolved in CH_2Cl_2. These were mixed directly and were stirred for about 30 min. This gave brown powder (powder sample). Powder sample was dried in vacuum overnight. Anal. Calcd for $C_{42}H_{28}N_6S_2Fe(0.6CH_2Cl_2)(C_2H_5OH)$: C, 65.7; H, 4.08; N, 9.66; S, 7.37%. Found: C, 64.5; H, 4.36; N, 9.39; S, 8.45%. Single crystals ($[Fe(NCS)_2(1,5\text{-bpna})_2\cdot(\text{toluene})]_n$) were

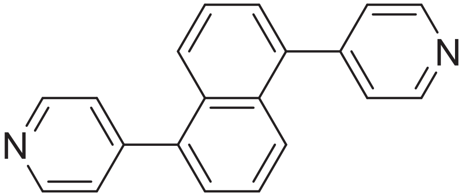

Scheme 1 1,5-Bis(4-pyridyl)naphthalene (1,5-bpna).

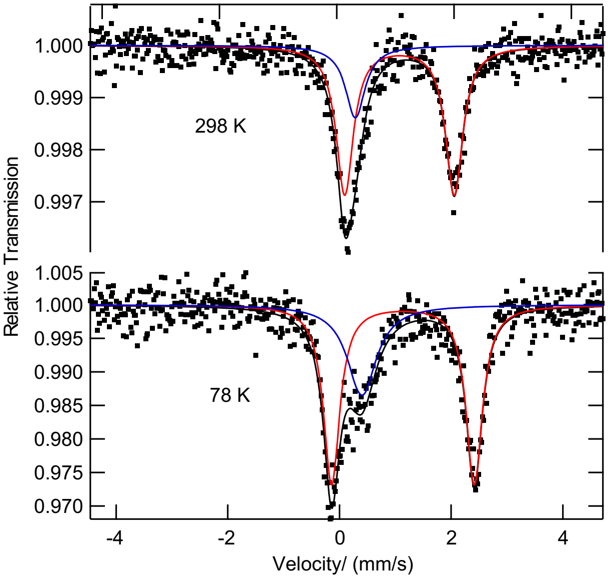

Fig. 1 ^{57}Fe Mössbauer spectra of [Fe(NCS)$_2$(1,5-bpna)$_2$•(0.6CH$_2$Cl$_2$)(C$_2$H$_5$OH)]$_n$ (powder sample)

obtained by diffusion method (top layer: FeSO$_4$•7H$_2$O and KNCS in EtOH, middle layer: EtOH and toluene, bottom layer: 1,5-bpna in toluene).

^{57}Fe Mössbauer spectroscopic measurement was performed at 78 K and room temperature with a ^{57}Co (Rh) radiation source moving in a constant acceleration mode on Wissel MB-500. The Mössbauer parameters were obtained by least-squares fitting to Lorentzian peaks using

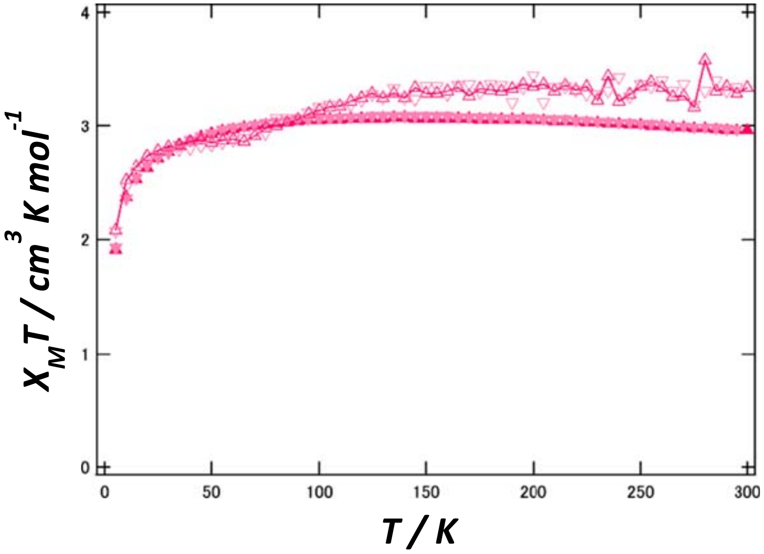

Fig. 2 Magnetic susceptibility for [Fe(NCS)$_2$(1,5-bpna)$_2$•(0.6CH$_2$Cl$_2$)(C$_2$H$_5$OH)]$_n$ (powder sample) and [Fe(NCS)$_2$(1,5-bpna)$_2$•(toluene)]$_n$. △ and ▽ show the increasing mode and decreasing mode, respectively, for powder sample. ▲ and ▼ show the increasing mode and decreasing mode, respectively, for [Fe(NCS)$_2$(1,5-bpna)$_2$•(toluene)]$_n$

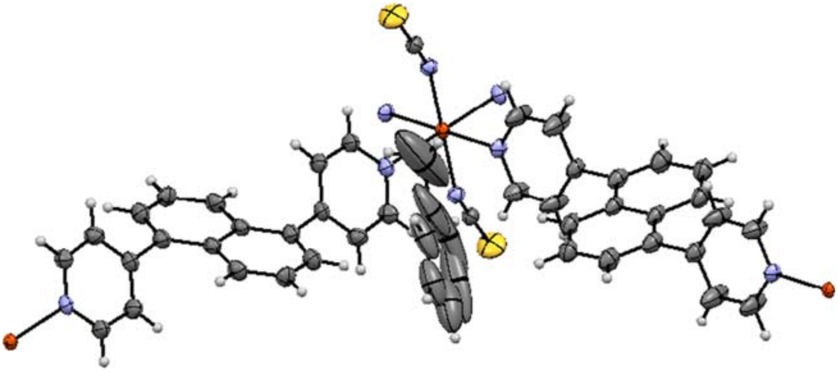

Fig. 3 Ortep drawing of $[Fe(NCS)_2(1,5\text{-bpna})_2\cdot(toluene)]_n$

NORMOS-90. The spectra were calibrated by the six lines of α-Fe, the center of which was taken as zero isomer shift. We recalculated the background of the spectrum at room temperature because the background was slightly inclined.

Magnetic susceptibility measurement was performed on Quantum Design MPMS-5S SQUID apparatus, magnetic field was 1000 Oe. The scan rate was 3 K/ min.

For single crystal X-ray diffraction analysis, all diffraction data were collected by using a Bruker SMART-APEX diffractometer equipped with CCD area detector and graphite-monochromated MoKα radiation ($\lambda = 0.71073$ Å, ω-scan mode). The structure was solved by direct method.

3 Results and discussion

Figure 1 shows ^{57}Fe Mössbauer spectra of the powder sample. Two species were observed at 78 K (IS = 1.14 mm/s, QS = 2.55 mm/s, Γ = 0.35 mm/s and IS = 0.41 mm/s, QS = 0.00 mm/s, Γ = 0.64 mm/s). One is Fe(II) HS state and the other is Fe(II) LS state. Two species were also observed at room temperature (IS = 1.07 mm/s, QS = 1.87 mm/s, Γ = 0.36 mm/s and IS = 0.32 mm/s, QS = 0.00 mm/s, Γ = 0.41 mm/s). The ratio of singlet decreased at room temperature (31% ➔ 22%).

The results of magnetic susceptibility are shown in Fig. 2. Slight decrease is observed at lower temperatures for the powder sample ($T_{1/2} = 100$ K). This shows that the powder sample shows incomplete SCO.

Table 1 Crystal data of $[Fe(NCS)_2(1,5\text{-bpna})_2\cdot(toluene)]_n$

Formula	$C_{49}H_{36}FeN_6S_2$	a / Å	9.1458(15)
Temperature / K	173	b / Å	16.317(3)
Crystal system	monoclinic	c / Å	16.169(3)
Space group	P 1 21/c 1	Z	4
Volume / Å^3	2324.3(7)	Goodness of fit	0.999
Size / mm	0.244*0.70*0.10	Color	Dark brown
R	0.0555	Fe-N(NCS) / Å	2.1091(17)
wR	0.1429	Fe-N(bpna) / Å	2.244(2), 2.240(3)

Figure 2 also shows the results of $[\mathrm{Fe(NCS)_2(1,5\text{-}bpna)_2{\bullet}(toluene)}]_n$. This shows temperature independent HS state. Figure 3 shows Ortep drawing of $[\mathrm{Fe(NCS)_2(1,5\text{-}bpna)_2{\bullet}(toluene)}]_n$. The assembled structure is 2D grid type. The crystal data are summarized in Table 1. Fe-N distances are 2.11 and 2.24 Å, showing HS state. The local structure around iron atom is shown in Fig. 4. This shows the parallel type of coordinated pyridines for $[\mathrm{Fe(NCS)_2(1,5\text{-}bpna)_2{\cdot}(toluene)}]_n$, which is consistent with SCO-off.

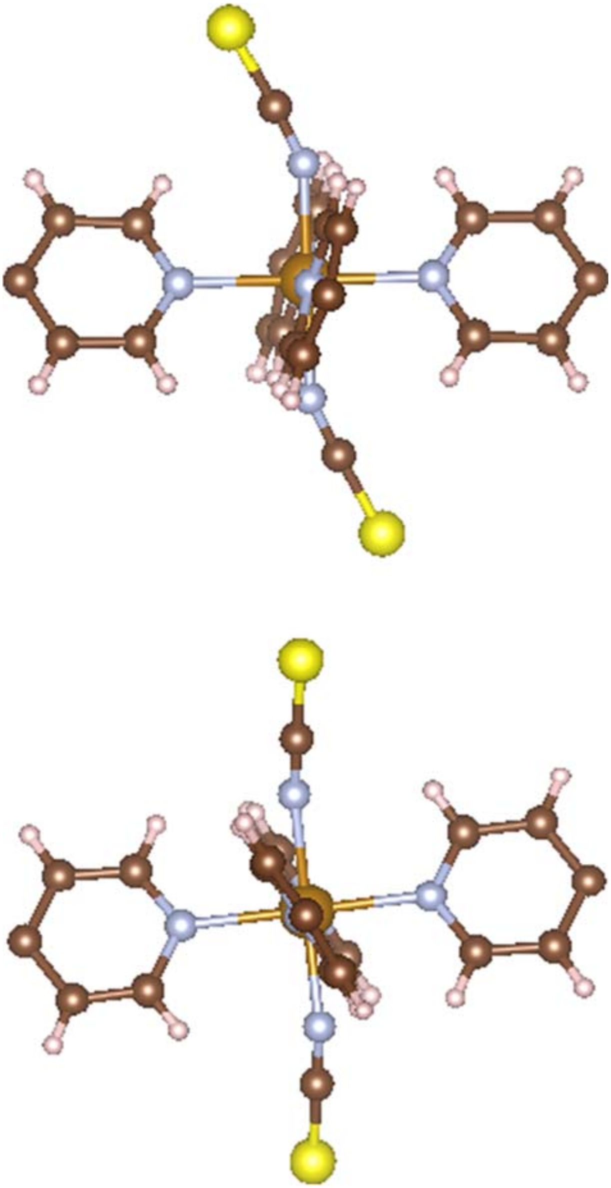

Fig. 4 Local structure around iron atom for $[\mathrm{Fe(NCS)_2(1,5\text{-}bpna)_2{\cdot}(toluene)}]_n$

The two shortest C(toluene)-H(naphthalene) distances are 2.758 and 2.979 Å, which are shorter than and almost the same with the sum of van der Waals radius (2.9 Å), respectively. This suggests the CH-π interaction between guest toluene and naphthalene in the bridging ligand. It is thought that CH-π interaction forced the unstable parallel structure and it becomes difficult for the complex to change the structure to become LS state with decreasing temperature. One of the possibilities which show incomplete SCO for powder sample is that the lack of CH-π interaction allows the slight approach of Fe-N distance.

4 Conclusion

We obtained $[Fe(NCS)_2(1,5\text{-bpna})_2\cdot(0.6CH_2Cl_2)(C_2H_5OH)]_n$ (powder sample) and $[Fe(NCS)_2(1,5\text{-bpna})_2\cdot(\text{toluene})]_n$. The CH-π interaction between toluene and bridging ligand forced the parallel local structure, showing SCO-off. On the other hand, if the toluene molecule is not, the local structure becomes slightly free, and the incomplete SCO appears. It was revealed from the present study that intermolecular interaction (CH-π interaction) has the roll of stabilization of parallel local structure around iron atom to destabilize the LS state in the Fe(II) assembled complexes.

References

1. *Spin Crossover in Transition Metal Compounds I*, Gütlich, P; Goodwin, H. A.Ed..; Springer-Verlag: Berlin, 2004.
2. Halder, G.J., Kepert, C.J., Moubaraki, B., Murray, K.S., Cashion, J.D.: Guest-dependent spin crossover in a nanoporous molecular framework material. Science. **2002, 298**, 1762–1765
3. Kaneko, M., Tokinobu, S., Nakashima, S.: Density functional study on spin-crossover phenomena of assembled complexes, $[Fe(NCX)_2(bpa)_2]_n$ (X = S, Se, BH_3; bpa = 1,2-bis(4-pyridyl)ethane). Chem. Lett. **42**, 1432–1434 (2013)
4. Kaneko, M., Nakashima, S.: Computational study on thermal spin-crossover behavior for coordination polymers possessing trans-$Fe(NCS)_2(pyridine)_4$ unit. Bull. Chen. Soc. Jpn. **88**, 1164–1170 (2015)
5. Wu, X.R., Shi, H.Y., Wei, R.J., Li, J., Zheng, L.S., Tao, J.: Coligand and solvent effects on the architectures and spin-crossover properties of (4,4)-connected Iron(II) coordination polymers. Inorg. Chem. **54**, 3773–3780 (2015)
6. Iwai, S., Yoshinami, K., Nakashima, N.: Structure and spin state of Iron(II) assembled complexes using 9,10-bis(4-pyridyl)anthracene as bridging ligand. Inorganics. **5**, 61 (2017)